Pathology - Research and Practice 215 (2019) 152376

Contents lists available at ScienceDirect

Pathology - Research and Practice

journal homepage: www.elsevier.com/locate/prp

Long non-coding RNA MIF-AS1 promotes breast cancer cell proliferation, migration and EMT process through regulating miR-1249-3p/HOXB8 axis

Jinhua Ding[1], Weizhu Wu[1,*], Jiahui Yang, Minhua Wu

Department of Thyroid and Breast, Ningbo Medical Center Lihuili Eastern Hospital/Taipei Medical University Ningbo Medical Center, Ningbo, Zhejiang Province, 315000, China

ARTICLE INFO

Keywords:
MIF-AS1
ceRNA
Breast cancer
miR-1249-3p
HOXB8

ABSTRACT

Breast cancer (BC) is one of the leading cause of cancer-related death among females worldwide. Mounting evidences indicate that long non-coding RNAs (lncRNAs) were involved in tumor progression by acting as either oncogenes or tumor suppressors in multiple cancers. In this study, we focused on the function and mechanism of lncRNA Migration Inhibitory Factor Antisense RNA 1 (MIF-AS1) in BC. qRT-PCR showed that MIF-AS1 was upregulated in BC tissues and cells. To detect its bio-function, a series of loss-of-function assays were carried out. Thereafter, we found that MIF-AS1 depletion inhibited BC cell proliferation, migration and epithelial-mesenchymal transition (EMT). Recently, increasing studies indicate that lncRNAs can function as competing endogenous RNAs (ceRNAs). Using bioinformatics analysis and luciferase reporter assay, we identified that MIF-AS1 regulated the level of Homeobox B8 (HOXB8) via binding to miR-1249-3p. Taken all together, our findings proved that MIF-AS1 acted as a ceRNA by modulating miR-1249-3p/HOXB8 axis in breast cancer. LncRNA MIF-AS1 might be a new biomarker and therapeutic target for BC patients.

1. Introduction

Breast cancer (BC) is one of the most prevalent malignancies and ranked the second leading cause of cancer-related death among females worldwide [4,9,31,32,35]. Although the combination of surgery and adjuvant therapy is constantly improved, BC is still characterized by high morbidity and unsatisfactory prognosis [7,23–25]. Therefore, the molecular mechanisms involved in the initiation and development of BC still need to be explored, which will contribute to finding new biomarkers or therapeutic strategies for BC patients.

As a sub-group of non-coding RNAs (ncRNAs) family, long non-coding RNAs (lncRNAs) are identified as a type of RNA molecules that are longer than 200 nucleotides and unable to code protein [36]. Recent years, lncRNAs have attracted more and more attentions due to their comprehensive regulatory roles in human diseases, particularly in tumors [34,38]. Increasing studies show that the dysregulation of lncRNAs plays a crucial role in regulating biological processes of tumors, including cell proliferation, migration and epithelial-mesenchymal transition (EMT) [11,20,22,44,45]. More importantly, lncRNAs usually exert functions by regulating gene expressions at multiple levels, such transcriptional, post-transcriptional or translational [1,16,29]. Some lncRNAs are located mainly in cytoplasm and can regulate gene expression levels post-transcriptionally. They are identified as competing endogenous RNAs (ceRNAs) to modulate the expressions of specific mRNAs through binding to miRNAs [2,3,5,27,42]. Based on previous studies, numerous lncRNAs were reported to regulate BC progress [12,18,26,30,39]. As an emerging lncRNA, migration inhibitory factor antisense RNA 1 (MIF-AS1) was reported to promote cell proliferation and reduce apoptosis in gastric cancer [19]. So far, no relevant report concerns the role of MIF-AS1 in BC. Therefore, this study aimed to explore the bio-function and mechanism of MIF-AS1 in BC.

In the study, MIF-AS1 was upregulated in BC and associated with poor prognosis in BC patients. To explore the function of MIF-AS1, we designed and conducted loss-of-function assays. Based on results, we determined the oncogenic role of MIF-AS1 in BC. Mechanistically, bioinformatics analysis and luciferase reporter assay were utilized to investigate the underlying mechanism that involved in the MIF-AS1-mediated development of BC. According to mechanism experiments, a new ceRNA network (MIF-AS1/miR-624-3p/HOXB8) was identified. Rescue assays were performed to confirm that MIF-AS1 promoted BC's development in a miR-624-3p/HOXB8 manner. In summary, our study provided a promising biomarker for the treatment of BC.

* Corresponding author.
E-mail address: WeizhuWu_er14@163.com (W. Wu).
[1] Contributed equally to this work.

https://doi.org/10.1016/j.prp.2019.03.005
Received 19 November 2018; Received in revised form 3 February 2019; Accepted 2 March 2019

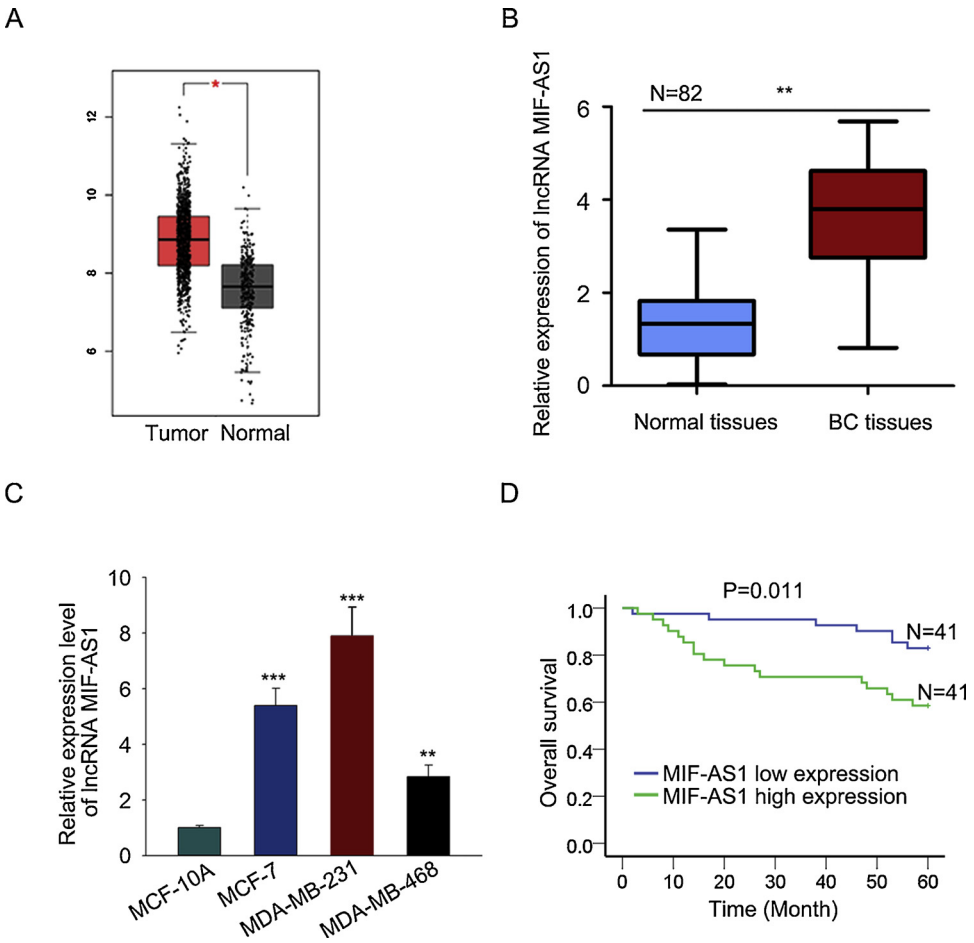

Fig. 1. Upregulation of MIF-AS1 BCE was associated with the patients' prognosis. A. Box plot presented the expression pattern of MIF-AS1 in TCGA database. Two horizontal lines represent the mean values. **B.** MIF-AS1 expression in tumor tissue and paired adjacent normal tissues. **C.** The expression level of MIF-AS1 was detected in three BC cell lines and a human mammary epithelial cell (MCF-10A). **D.** The survival curve revealed the correlation between different expressions of MIF-AS1 and the prognosis of BC patients. $^{*}P < 0.05$, $^{**}P < 0.01$ and $^{***}P < 0.001$ indicate data are statistically significant.

Table 1
Correlation between lncRNA MIF-AS1 Expression and Clinical Features. (n = 82).

Variable	MIF-AS1 Expression		P-value
	low	high	
Age			
< 50	16	13	0.645
≥ 50	25	28	
Menopause			
pre	32	30	0.798
post	9	11	
Tumor size			
≤ 2.0	25	23	0.823
> 2.0	16	18	
Node status			
Negative	27	29	0.813
Positive	14	12	
TNM			
I + II	24	10	0.003**
III	17	31	
HR status			
Negative	30	33	0.002**
Positive	11	8	
HER-2 status			
Negative	25	10	0.602
Positive	16	31	

Low/high expression was obtained by the sample mean. Pearson χ^2 test. $^{**}P < 0.01$ was considered statistically significant.

2. Materials and methods

2.1. Clinical specimens

A total of 82 patients with breast cancer were recruited for this study from August 2012 to July 2017 at Ningbo Medical Center Lihuili Eastern Hospital. Patients free from chemotherapy and radiotherapy prior to mastectomy were qualified for this study. Cancerous and paired normal paracancerous tissues (3–5 cm distal to the edge of tumor) of 82 cases were excised during the surgery and snap-frozen in liquid nitrogen. Tissue specimens were then stored at −80 °C until required. The written informed consents from 82 patients were reviewed and approved by the Ethic Committee of Ningbo Medical Center Lihuili Eastern Hospital (approval number: DYLL2012086).

2.2. Cell lines and culture

Human mammary epithelial cell line (MCF-10A) and three human breast cancer cell lines, including MCF-7, MDA-MB-231 and MDA-MB-468, were all purchased from American Type Culture Collection (ATCC, Rockville, Maryland, USA). Cell lines grown routinely in Dulbecco's Modified Eagle's Medium (DMEM, Invitrogen, Carlsbad, CA, USA) at 37 °C in a humidified incubator containing 5% CO_2. 10% fetal bovine serum (FBS, Gibco, Carlsbad, USA) and double antibiotics (100 U/ml penicillin and 100 μg/ml streptomycin, Invitrogen, USA) were used to supplement culture medium. The replacement of medium was performed every third day. Cells were passaged as soon as attachment rate reached approximately 80–90%.

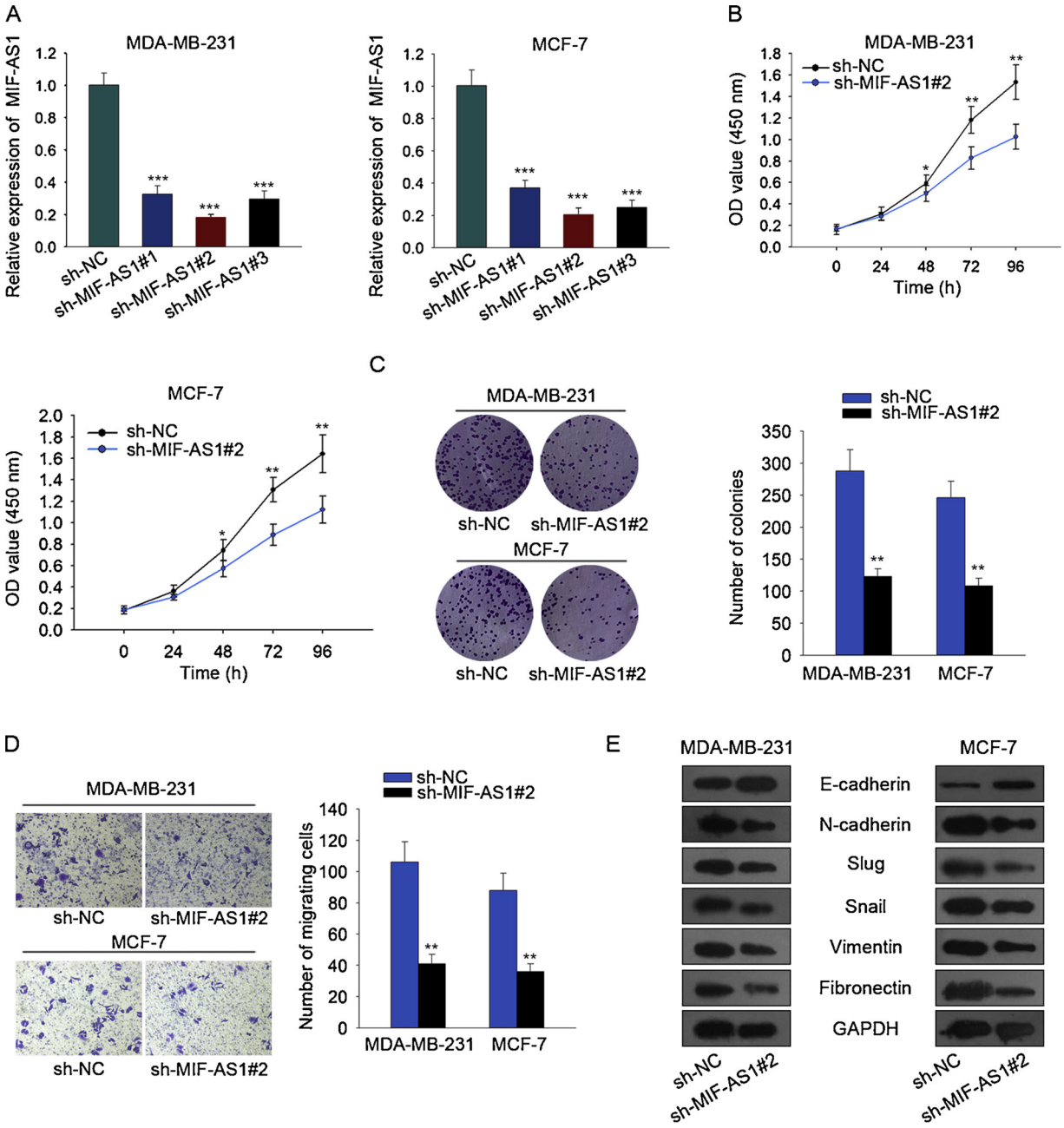

Fig. 2. MIF-AS1 knockdown inhibited cell proliferation, migration and EMT in BC. A. MIF-AS1 was silenced by specific shRNAs (sh-MIF-AS1#1, sh-MIF-AS1#2, sh-MIF-AS1#3) in MDA-MB-231 and MCF-7 cell lines. **B–C.** CCK-8 assay and colony formation assay were used to detect the effect of MIF-AS1 knockdown on BC cell viability. **D.** Transwell migration assay revealed how MIF-AS1 knockdown affected tumor cell migratory ability. **E.** Western blot assay was conducted to detect the protein levels of EMT markers in response to the depletion of MIF-AS1. $^{*}P < 0.05$, $^{**}P < 0.01$ and $^{***}P < 0.001$ indicate data are statistically significant.

2.3. RNA extraction and quantitative real-time polymerase chain reaction (qRT-PCR)

Total RNA was extracted from specimens and cultured cells using Trizol reagent (Life Technologies, CA, USA) in accordance with user manual. A spectrophotometer (Bio-Rad, Hercules, CA, USA) was utilized to assess the concentration and purity of the extracted RNA. Afterwards, the RNAs were converted into complementary DNA (cDNA) with specific primers based on the instruction book of PrimeScript™ RT Master Mix Kit (Takara, Tokyo, Japan). SYBR® Green PCR Kit (Takara, Japan) was used to conduct quantitative real-time PCR on Thermal Cycler CFX6 System (Bio-Rad, California, USA). The thermal cycling parameters were described as below: denatured at 95 °C for 10 min, following 40 cycles of denaturation at 95 °C for 30 s, annealing at 60 °C for 30 s and extension at 72 °C for 1 min. The relative expression levels of RNAs were quantified by $2^{-\Delta\Delta Ct}$ method, normalizing to GAPDH or U6. The primers used for qRT-PCR were described as below: MIF-AS1 forward primer: 5′-CCCGACAAAAAGCCCAACTG-3′, MIF-AS1 reverse primer: 5′-CCCCGTTTTCACGCATTTGT-3′; miR-1249-3p forward primer: 5′-ACGAAATTAACCTCCGGCTTTA-3′; miR-1249-3p reverse primer: 5′-CTCTACAGCTATATTGCCAGCCA-3′; HOXB8 forward primer: 5′-TTGGCTGGTGGGTTGACATT-3′, HOXB8 reverse primer: 5′-TTCCAGGATTTCTGGGCCAC-3′; GAPDH forward primer: 5′-ATTTC TCCTCCGGGTGATGC-3′, GAPDH reverse primer: 5′-GCCATTTTGCGG TGGAAATGT-3′; U6 forward primer: 5′- GCAGACCGTTCGTCAAC CTA-3′, U6 reverse primer: 5′- AATTCTGTTTGCGGTGCGTC-3′.

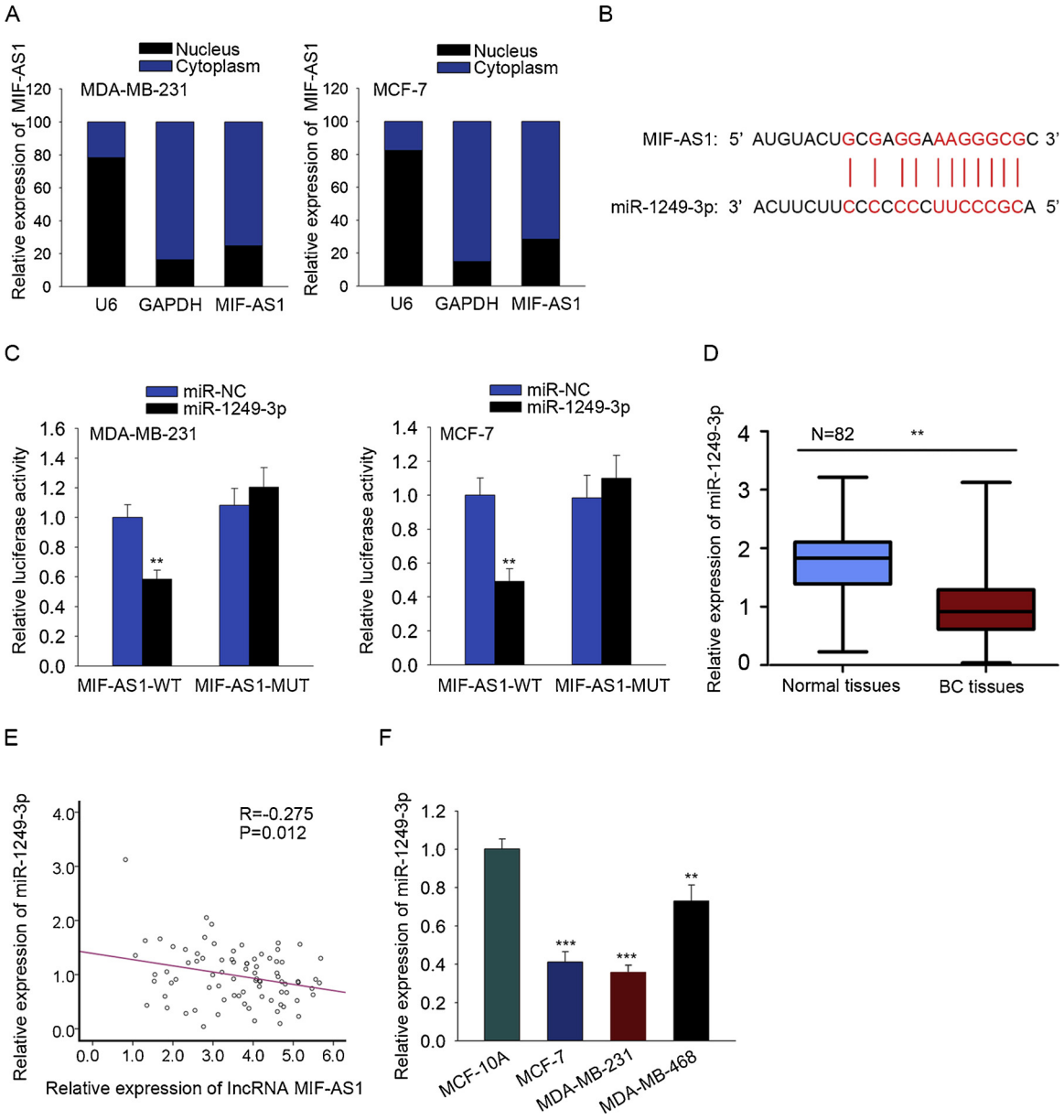

Fig. 3. MIF-AS1 acted as a sponge for miR-1249-3p in BC cells. A. The location of MIF-AS1 in MDA-MB-231 and MCF-7 cell lines was detected by nuclear-cytoplasmic fractionation. **B.** The putative binding sites of MIF-AS1 and miR-1249-3p were predicted using Starbase prediction website. **C.** Luciferase reporter assay was performed to verify whether MIF-AS1 could bind to miR-1249-3p. **D.** qRT-PCR was applied to analyze miR-1249-3p expression level in breast cancer tissues. **E.** Spearman's correlation analysis revealed the negative relation between MIF-AS1 and miR-1249-3p. **F.** The different expression levels of miR-1249-3p in BC cell lines. $^{*}P < 0.05$, $^{**}P < 0.01$ and $^{***}P < 0.001$ indicate data are statistically significant.

2.4. Cell transfection

The short hairpin RNAs (shRNAs) against MIF-AS1 (termed sh-MIF-AS1#1, sh-MIF-AS1#2, sh-MIF-AS1#3), the shRNA targeted to HOXB8 (termed sh-HOXB8), pcDNA 3.1 vector specific to MIF-AS1 (termed MIF-AS1) and relative controls (sh-NC, empty pcDNA vector) were designed and synthesized by Genechem Company (Shanghai, China). The miR-1249-3p mimics (termed miR-1249-3p) and corresponding control (termed miR-NC) were simultaneously synthesized by Genechem. MDA-MB-231 and MCF-7 cell lines were seeded into 6-well plates in DMEM containing 10% FBS, followed by incubation at 37 °C. Transfection was performed using Lipofectamine 2000 (Invitrogen, Carlsbad, CA, USA). 48 h after transfection, cells were harvested for subsequent experiments. Each procedure of transfection assay was repeated for more than three times.

2.5. Nuclear-cytoplasmic fractionation

Nuclear-cytoplasmic fractionation assay was performed using PARIS™ Kit (Invitrogen, CA, USA) in line with the specification provided by supplier. Firstly, cells were lysed in cell fractionation solution to separate the nuclear and cytoplasmic fractions. Afterwards, cell supernatant was transferred into a fresh RNase-free tube, the remaining lysate was rinsed with cell fractionation buffer. After centrifugation, the lysate was subjected to cell disruption buffer to obtain the cell nucleus, following incubation on ice to remove the residual cytoplasmic fraction. Thereafter, lysates and cell supernatant were re-suspended in 2 × lysis/binding and equal volume of ethyl alcohol. After elution, the cytoplasmic and nuclear RNAs were extracted using TRIzol (Life Technologies, CA, USA). U6 and GAPDH were seen as the nuclear and cytoplasmic internal references, respectively. Experiment was conducted independently in triplicate.

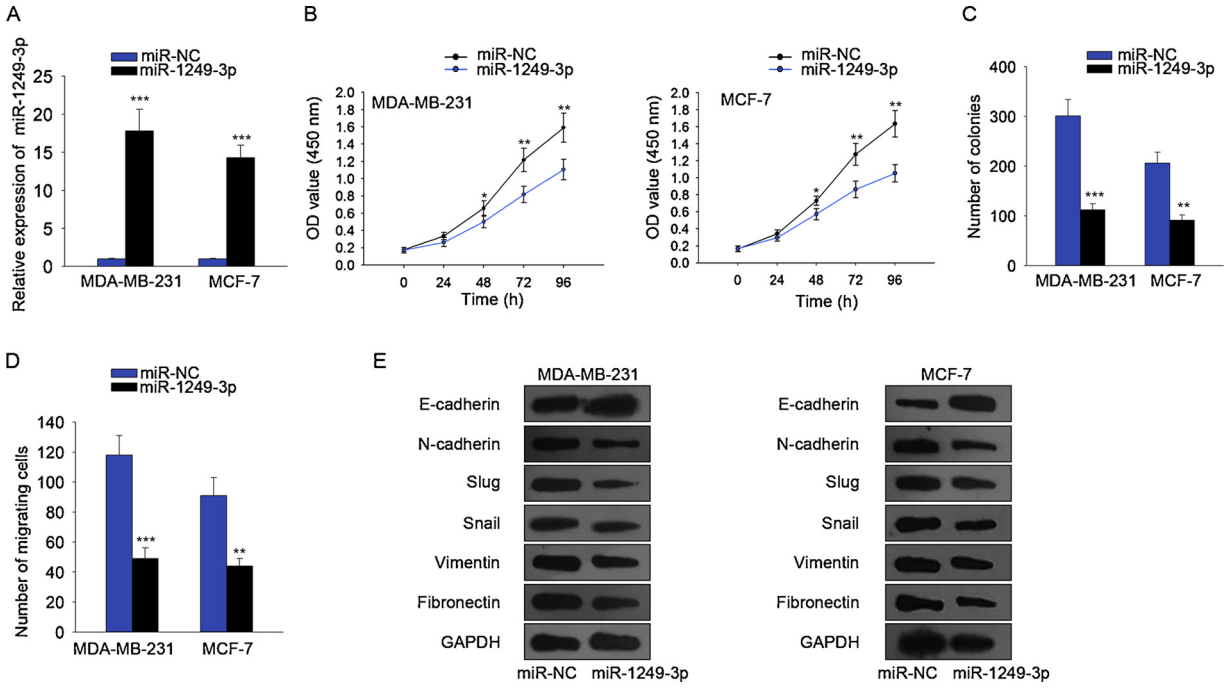

Fig. 4. Influence of miR-1249-3p overexpression on the BC cell viability, migration and EMT process. A. qRT-PCR revealed that the expression level of miR-1249-3p was enhanced successfully in MDA-MB-231 and MCF-7 cell lines. **B–C.** After transfection with miR-1249-3p mimics, BC cell proliferative ability was assessed by CCK-8 assay and colony formation assay. **D.** Transwell assay demonstrated the impact of miR-1249-3p mimics on the BC cell migratory capacity. **E.** The protein levels of EMT markers influenced by miR-1249-3p mimics were detected by western blot assay. $^{*}P < 0.05$, $^{**}P < 0.01$ and $^{***}P < 0.001$ indicate data are statistically significant.

2.6. Luciferase reporter assay

The wild-type and mutant reporter plasmids of MIF-AS1 (termed MIF-AS1-WT/MUT) and HOXB8 (termed HOXB8-WT/MUT) were constructed by Promega Corporation (Fitchburg, Wisconsin, USA). Luciferase reporter assay was performed using a Dual Luciferase reporter assay system (Promega). MDA-MB-231 and MCF-7 cell lines were seeded into 96-well plates and cultured until cell attachment rate reached to 80%. Thereafter, MIF-AS1-WT and MIF-AS1-MUT were co-transfected with miR-1249-3p mimics and NC using Lipofectamine 2000 (Invitrogen, Carlsbad, CA, USA). HOXB8-WT and HOXB8-MUT were co-transfected with miR-1249-3p mimics, mimics plus pcDNA-MIF-AS1 and negative control, respectively. 48 h later, luciferase activities were monitored and normalized to Renilla. The replication of this assay was performed for at least three times.

2.7. Cell counting Kit-8 (CCK-8) assay

To estimate the cell viability of the MDA-MB-231 and MCF-7 cell lines, CCK-8 assay was performed in accordance with user's guidebook. Cells were seeded into 96-well plates (2×10^3 cells per well) supplemented with complete culture medium. Afterwards, cells were transfected and incubated at 37 °C with 5% CO_2. 12 h later, CCK-8 solution (Dojindo Molecular Technologies, Inc., Kumamoto, Japan) were added to each well, following further incubation at 37 °C for 2 h. Cell viability was determined via measuring the absorbance at 450 nm using a microplate reader (Bio-Rad, Hercules, CA, USA) at various time points (24 h, 48 h, 72 h and 96 h). CCK-8 assay was carried out independently for three times.

2.8. Colony formation assay

For colony formation assay, MDA-MB-231 and MCF-7 cell lines were transfected for 48 h and placed into 6-well plates with medium at a density of 1×10^3 cells/well. Cells were cultured in an incubator at 37 °C with 5% CO_2. Medium was replaced every three days. The incubation was terminated after two weeks. Subsequently, cells were washed three times with the phosphate-buffered saline (PBS, Invitrogen, CA, USA). After fixation with 4% paraformaldehyde for 30 min, remaining liquid was removed. Cells were stained with 0.1% crystal violet for 30 min. Next, excessive crystal violet solution was removed, cells were rinsed with PBS until the solution became clear. Visible colonies were counted manually and recorded. Colony formation assay was performed more than three times.

2.9. Transwell migration assay

The transfected cells were harvested and seeded onto the upper chamber of 24-well transwell plates (8-μm-pore size). Lower chamber was filled with DMEM supplemented with 10% FBS. After incubation at 37 °C for 48 h, cells remaining on the upper surface were removed with cotton swabs, whereas cells in the lower chamber were fixed with 4% paraformaldehyde and stained with 0.1% crystal violet solution. Cells migrating through the membrane were counted at five random fields under optical microscope (magnification ×200, Thermo, CA, USA). Three replicates of each group were conducted.

2.10. Western blot assay

Total protein was isolated from cell lines using RIPA buffer reagent (Sigma, St. Louis, MO, USA) containing proteinase. Each protein band was separated by the sodium dodecyl sulfate polyacrylamide gel electrophoresis (SDS-PAGE, Thermo Fisher Scientific, Inc. Rochester, New York, USA), then transferred onto polyvinylidene fluoride membrane (PVDF, Millipore, Billerica, MA, USA). Thereafter, PVDF membranes were blocked with 5% bovine serum albumin solution (BSA, Beyotime, Shanghai, China) in Tris buffered saline with Tween 20 (TBST) at room temperature for two hours. The membranes were incubated with specific primary antibodies (at 1:1000 dilution) against E-cadherin (Abcam, Santa Cruz Biotechnology, Inc. Dallas, TX, USA, ab76055), N-

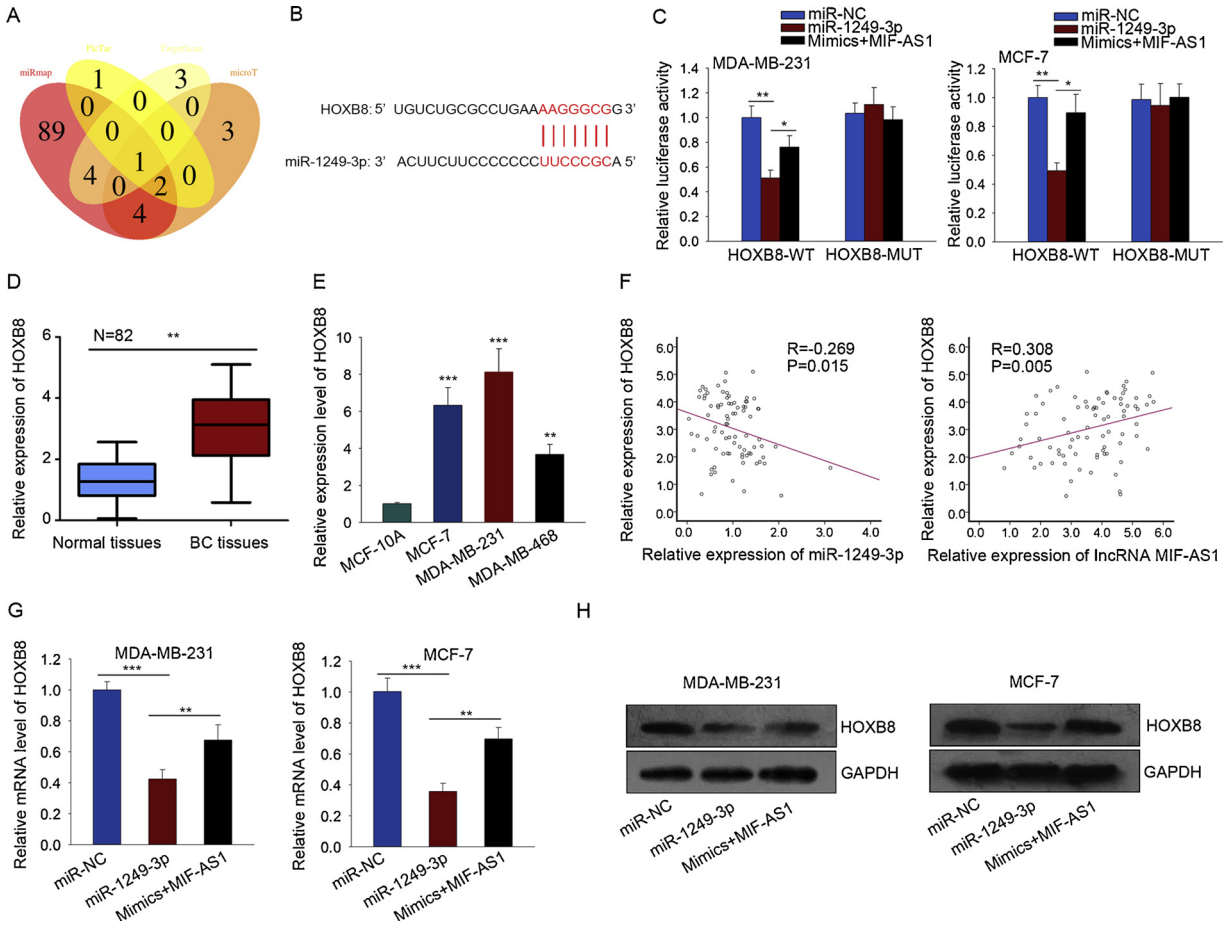

Fig. 5. MIF-AS1 competed with HOXB8 for binding to miR-1249-3p. A. Bioinformatics analysis (Targetscan, microT, miRmap and PicTar) was used to screen the potential target genes of miR-1249-3p. **B.** The putative binding sites of HOXB8 and miR-1249-3p were obtained. **C.** Luciferase reporter assay was used to identify the binding sites of HOXB8 and miR-1249-3p. **D–E.** qRT-PCR was applied to detect the expression levels of HOXB8 in breast cancer tissues and cells. **F.** Spearman's correlation analysis was performed to evaluate the relation between HOXB8 and MIF-AS1 or miR-1249-3p. **G.** The coordinated regulation of MIF-AS1 and miR-1249-3p to HOXB8 expression level was measured by qRT-PCR. **H.** The protein level of HOXB8 was measured by western blot assay. $^{*}P < 0.05$, $^{**}P < 0.01$ and $^{***}P < 0.001$ indicate data are statistically significant.

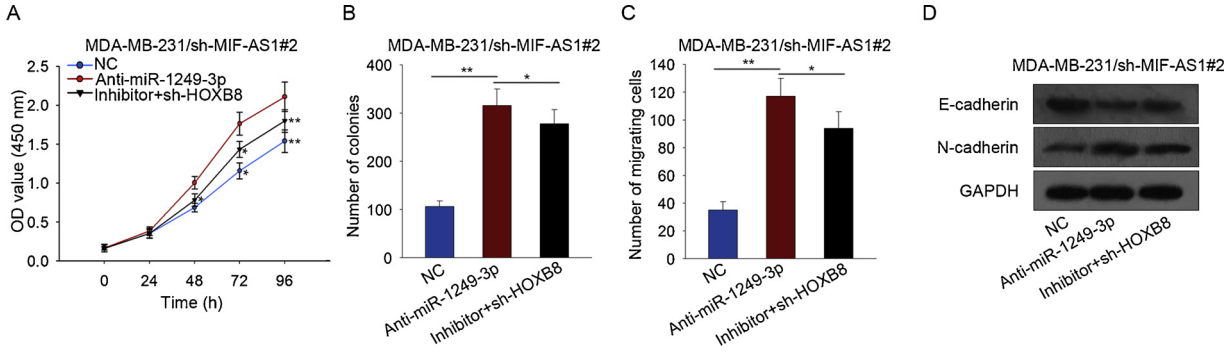

Fig. 6. The miR-1249-3p/HOXB8 axis was involved in the oncogenic function of MIF-AS1 in BC cell. A–B. CCK-8 and colony formation assays were conducted to detect the impact of anti-miR-1249-3p or anti-miR-1249-3p plus HOXB8 knockdown on sh-MIF-AS1#2-mediated breast cancer cell viability. **C.** The migratory cells were quantified after treatment separately with silencing miR-1249-3p and silencing both miR-1249-3p and HOXB8. **D.** The sh-MIF-AS1#2-mediated protein levels of EMT markers were effected by miR-1249-3p inhibitor or the combination of miR-1249-3p inhibitor and HOXB8 knockdown. $^{*}P < 0.05$, $^{**}P < 0.01$ indicate that data are statistically significant.

cadherin (Abcam, ab18203), HOXB8 (Abcam, ab125727) and GAPDH (Abcam, ab9485) at 4 °C overnight. After rinsing with TBST, membranes were incubated with horseradish peroxidase (HRP)-conjugated secondary antibodies (at 1:2000 dilution) at room temperature for two hours. Finally, the protein bands were visualized using the enhanced chemiluminescence reagent (ECL, Bio-Rad, Hercules, CA, USA). GAPDH was seen as an internal reference. Results were determined after performing experiment for three times.

2.11. Bioinformatics analysis

The expression of MIF-AS1 in BC samples were downloaded from Cancer Genome Atlas (TCGA) database (http://gepia.cancer-pku.cn/index.html). Starbase version 2.0 (http://starbase.sysu.edu.cn/) was

applied to predict the potential miRNAs regulated by MIF-AS1. Bioinformatics analysis tools (TargetScan, microT, miRmap and PicTar) were utilized to search out the putative targets of miR-1249-3p.

2.12. Statistical analysis

In the study, each experimental procedure was repeated independently at least three times. Data were expressed as mean ± standard deviation (SD) and analyzed using SPSS version 22.0 software (IBM, Chicago, IL, USA). One-way analysis of variance (ANOVA) or two-tailed Student's *t*-test was utilized to compare the group differences. The survival curve was plotted by Kaplan-Meier method and analyzed by log-rank test. Difference were significant when p values were less than 0.05.

3. Results

3.1. Upregulation of MIF-AS1 BCE was associated with the patients' prognosis

According to TCGA database (http://gepia.cancer-pku.cn/index.html), we found that the expression level of MIF-AS1 in BC tissues was much higher than that in normal tissues (Fig. 1A). Moreover, the expression level of MIF-AS1 was detected in tissues collected from 82 BCE patients. Comparing with normal tissues, MIF-AS1 was prominently upregulated in tumor tissues (Fig. 1B), which was consistent with TCGA data analysis. As illustrated in Fig. 1C, the expression level of MIF-AS1 in BC cell lines (MCF-7, MDA-MB-231 and MDA-MB-468) were obviously more abundant compared to that in human mammary epithelial cell (MCF-10A). Based on the mean expression level of MIF-AS1 in 82 BCE tissues, all patient samples were divided into MIF-AS1 high or low groups. Through analyzing the correlation between MIF-AS1 expression and clinicopathological features of BC, we observed that the high expression of MIF-AS1 was closely related to the advanced BC TNM stage, whereas no significant relations to other clinical features (Table 1). Besides, we plotted survival curve using Kaplan-Meier method and log-rank test. We found that the high expression level of MIF-AS1 was closely associated with poor overall survival (OS) of patients with BC (Fig. 1D). Therefore, we hypothesized the regulatory role of MIF-AS1 in BC progression.

3.2. MIF-AS1 knockdown inhibited cell proliferation, migration and EMT in BC

In order to explore the biological function of MIF-AS1 in BC, loss-of-function assays were carried out. According to Fig. 1C, MIF-AS1 expression levels were highest in MDA-MB-231 and MCF-7 cell lines. Therefore, the two cells were chosen for subsequent experiments. qRT-PCR detection indicated that MIF-AS1 was efficiently silenced via transfection with the short hairpin RNAs specific to MIF-AS1 (sh-MIF-AS1#1, sh-MIF-AS1#2, sh-MIF-AS1#3). As illustrated in Fig. 2A, MIF-AS1 expression level was reduced most efficiently by sh-MIF-AS1#2 compared to sh-MIF-AS1#1 and sh-MIF-AS1#3. With that, sh-MIF-AS1#2 was chosen for subsequent functional assays. CCK-8 assay indicated that MIF-AS1 knockdown efficiently repressed cell viability (Fig. 2B). Additionally, the visible colonies were decreased in response to transfection with sh-MIF-AS1#2 (Fig. 2C). Next, Results of transwell assay suggested that silencing of MIF-AS1the capacity of cells to migrate (Fig. 2D). Thus, we further explored whether MIF-AS1 could alter the protein levels of EMT-related markers. Western blot assay showed that the inhibition of MIF-AS1 enhanced E-cadherin protein level and decreased the levels of N-cadherin, Slug, Snail, Vimentin and Fibronectin (Fig. 2E). Thus, the oncogenic role of MIF-AS1 in BC progression was determined.

3.3. MIF-AS1 acted as a sponge for miR-1249-3p in BC cells

Generally, lncRNAs can act as competing endogenous RNAs (ceRNAs) to sequester miRNAs, contributing to the releasing of corresponding miRNAs-targeted mRNAs transcripts [12,28]. This notion prompted us to further investigate whether MIF-AS1 could function as a ceRNA in BC cells. Firstly, nuclear-cytoplasmic fractionation assay identified that MIF-AS1 was largely enriched in the cytoplasm of MDA-MB-231 and MCF-7 cell lines (Fig. 3A). Thus, MIF-AS1 can regulate gene expression at post-transcription level. Then, we searched for miRNAs that contains complementary base pairs with MIF-AS1 using the bioinformatics prediction tool. Data showed that five miRNAs containing putative binding sites with MIF-AS1, among which, miR-1249-3p has not been reported in breast cancer. With that, we focused on miR-1249-3p in the following experiments. The putative binding sites of MIF-AS1 and miR-1249-3p were shown in Fig. 3**B**. Luciferase reporter assay revealed that miR-1249-3p overexpression markedly reduced the luciferase intensity of wild-type MIF-AS1 (MIF-AS1-WT), rather than that of mutant MIF-AS2 (MIF-AS1-MUT) (Fig. 3C). In contrast to MIF-AS1, qRT-PCR showed that miR-1249-3p was notably downregulated in BC tissues (Fig. 3D). As displayed in Fig. 3E, we found the negative relevance between MIF-AS1 expression and miR-1249-3p expression. Besides, we examined relative low expression level of miR-1249-3p in BC cells (Fig. 3F). Furthermore, knockdown of MIF-AS1 strengthened the expression level of miR-1249-3p in BC cells. The specific reaction condition for miR-1249-3p expression in MIF-AS1-downregulated BC cells was observed in a time-dependent manner (Supplementary Fig. 1A).

3.4. Influence of miR-1249-3p overexpression on the BC cell viability, migration and EMT process

To detect the biological function of miR-1249-3p in breast cancer, we overexpressed miR-1249-3p in MDA-MB-231 and MCF-7 cells (Fig. 4A). CCK-8 assay and colony formation assay showed that overexpression of miR-1249-3p dramatically inhibited cancer cell proliferative ability (Fig. 4**B-C**). Transwell assay demonstrated that strengthened miR-1249-3p led to a reduction of migratory cells (Fig. 4**D-E**). Moreover, the enhanced miR-1249-3p expression led to the increased level of E-cadherin and decreased level of N-cadherin, Slug, Snail, Vimentin and Fibronectin (Fig. 4F), indicating the suppressive role of miR-1249-3p overexpression in EMT process. Additionally, we overexpressed MIF-AS1 and silenced miR-1249-3p in MCF-10A cells (Supplementary Fig. 1B) and found that there were no changes in cell viability (Supplementary Fig. 1C).

3.5. MIF-AS1 competed with HOXB8 for binding to miR-1249-3p

Using bioinformatics analysis tools (TargetScan, microT, miRmap and PicTar), we found that HOXB8 was the putative downstream target gene of miR-1249-3p (Fig. 5A). MiR-1249-3p was found to have complementary base pairing with HOXB8 3′UTR (Fig. 5B). Luciferase reporter assay was performed and indicated that the luciferase intensity of HOXB8-WT was strongly suppressed by miR-1249-3p mimics (termed miR-1249-3p or mimics), but partly recovered via enhancing MIF-AS1 expression (Fig. 5C). Nevertheless, there was no significant effect on HOXB8-MUT. Besides, qRT-PCR testified that HOXB8 was upregulated in breast cancer tissues and cell lines (Fig. 5**D-E**). Correlation analysis demonstrated the negative relevance between HOXB8 expression and miR-1249-3p expression as well as the positive relevance between HOXB8 expression and MIF-AS1 expression (Fig. 5F). What's more, it is observed that miR-1249-3p mimics downregulated the mRNA and protein levels of HOXB8, which was restored by MIF-AS1 overexpression (Fig. 5**G-H**).

3.6. MiR-1249-3p/HOXB8 axis was involved in the oncogenic function of MIF-AS1 in BC cell

For purpose of further verifying that MIF-AS1 promoted BC cell proliferation, migration and EMT process through miR-1249-3p/HOXB8 axis, we designed and performed rescue assays in MDA-MB-231 cells. Cells stably transfected with sh-MIF-AS1#2 were taken as the negative control (termed NC). On the basis of MIF-AS1 knockdown, cells were co-transfected with miR-1249-3p inhibitor or inhibitor + sh−HOXB8. CCK-8 and colony formation assays demonstrated that anti-miR-1249-3p improved the sh-MIF-AS1#2-mediated cell proliferative ability, but this favorable effect was attenuated in response to HOXB8 knockdown (Fig. 6**A-B**). By comparison to the NC group, the anti-miR-1249-3p-induced cell migration was abrogated by inhibiting HOXB8 expression (Fig. 6**C-D**). What's more, the sh-MIF-AS1#2-mediated N-cadherin protein level was enhanced after repressing miR-1249-3p, but reversed partially by inhibiting HOXB8. The opposite impact was observed in the level's alteration of E-cadherin. Western blot assay revealed that sh-MIF-AS1#2-mediated EMT process was accelerated by silencing miR-1249-3p, but this acceleration was attenuated after suppressing HOXB8 expression (Fig. 6E).

4. Discussion

Breast cancer includes four subtypes (basal-like, HER2+, luminal A and luminal B). Statistically, HER2 + BC is acknowledged as the highly aggressive breast cancer subtype [15]. Up till now, surgery remains a mainstay therapy for BC [14]. Early diagnosis via biomarkers is the key to decrease the morbidity and mortality of patients with BC. Although BC development is an elusive and complex process, a great number of lncRNAs were reported to involve in BC biological processes, including cell proliferation, migration and epithelial-mesenchymal transition (EMT) [10,17,40]. It has been proved that lncRNAs are of great significance for breast cancer development. Hence, this study focused on a certain lncRNA and aimed to explore functional lncRNAs in BC.

MIF-AS1, a new-found lncRNA, was reported to exert an oncogenic role in gastric cancer by Linhai Li et al. [19]. Based on TCGA dataset, MIF-AS1 was expressed higher in BC tissues. To our knowledge, it has not been studied in BC. Thus, our present study revealed the role of MIF-AS1 in BC progression. The aberrant expression of MIF-AS1 indicated the potential involvement of MIF-AS1 in BC development. What's more, we found that the high expression level of MIF-AS1 was closely related to the poor overall survival rate of BC patients. Thus, investigating the specific role of MIF-AS1 in BC progression is significant. Meanwhile, it prompted us to further investigate the biological function of MIF-AS1 in BC. Loss-of-function assays revealed that knockdown of MIF-AS1 inhibited BC cell proliferation, migration and epithelial-mesenchymal transition (EMT). With that, we concluded that MIF-AS1 functioned as an oncogene in breast cancer and it might predict a poor prognosis value for BC patients.

A growing number of studies showed that lncRNAs can act as competing endogenous RNAs (ceRNAs) to modulate mRNAs by competing for shared miRNAs [6,13,33,37,41,43]. For this reason, the ceRNA mechanism was given a great concern in the present study. With the help of online bioinformatics analysis, miR-1249-3p was screened out to do duty for a connecting carrier, targeting both MIF-AS1 and HOXB8. Luciferase reporter assays provided new evidences that both MIF-AS1 and HOXB8 could bind to miR-1249-3p in BC cells. In addition, MIF-AS1 could promote both mRNA level and protein level of HOXB8 through competitively absorbing miR-1249-3p. To detect the function of miR-1249-3p in BC cellular processes, we overexpressed it for gain-of function assays. Intriguingly, upregulation of miR-1249-3p suppressed cell migration and proliferation, reversed EMT progress efficiently. Moreover, previous reports have elucidated that HOXB8 is an oncogene in colorectal cancer [21] and gastric cancer [8]. In current study, we found that HOXB8 promoted cell proliferation and migration in MIF-AS1-downregulated BC cells. According to the results of rescue assays, we confirmed that miR-1249-3p/HOXB8 axis involved in MIF-AS1-mediated BC progression. On the whole, we drew a conclusion that a new MIF-AS1-mediated ceRNA network was identified in breast cancer.

In present study, we provided the evidence that MIF-AS1 exerts an oncogene in BC and contributes to BC cell viability, migration and EMT process. Particularly, we found a MIF-AS1/miR-1249-3p/HOXB8 pathway that conduced to initiation and development of BC. These findings enrich the theory of knowledge about the underlying molecular mechanism of MIF-AS1, providing a new potential biomarker and therapeutic target for patients with breast cancer. Further mechanism associated with the function of MIF-AS1 in BC will be studied in future.

Fund

This study was supported by the Individualized Endocrine Therapy for Luminal Breast Cancer (Fund number: 2015C0003), Effect of Autophagy on Anti-Breast Cancer of 2-Methoxyestradiol and its Mechanism (Fund number: 2018KY729) and Clinical and Curative Effects Prediction of Taxol with or without Carboplatin in the Adjuvant Chemotherapy of Triple-Negative Breast Cancer (Fund number: 2018KY724).

Authors' contributions

Jinhua Ding and Weizhu Wu were in charge of designing and carrying out this study. Jiahui Yang was responsible for the collection of experimental materials and the records of experimental results. Minhua Wu took charge of statistical analysis and article writing. Each author conduced to this study and provided valuable advice for this manuscript.

Conflicts and interests

Authors declare that they have no conflicts of interests.

Acknowledgement

The authors sincerely appreciate all members participated in this study.

Appendix A. Supplementary data

Supplementary material related to this article can be found, in the online version, at doi:https://doi.org/10.1016/j.prp.2019.03.005.

References

[1] P.J. Batista, H.Y. Chang, Long noncoding RNAs: cellular address codes in development and disease, Cell 152 (2013) 1298–1307.
[2] C. Cao, T. Zhang, D. Zhang, L. Xie, X. Zou, L. Lei, D. Wu, L. Liu, The long non-coding RNA, SNHG6-003, functions as a competing endogenous RNA to promote the progression of hepatocellular carcinoma, Oncogene (2016).
[3] D.L. Chen, Y.X. Lu, J.X. Zhang, X.L. Wei, F. Wang, Z.L. Zeng, Z.Z. Pan, Y.F. Yuan, F.H. Wang, H. Pelicano, P.J. Chiao, P. Huang, D. Xie, Y.H. Li, H.Q. Ju, R.H. Xu, Long non-coding RNA UICLM promotes colorectal cancer liver metastasis by acting as a ceRNA for microRNA-215 to regulate ZEB2 expression, Theranostics 7 (2017) 4836–4849.
[4] W. Chen, R. Zheng, P.D. Baade, S. Zhang, H. Zeng, F. Bray, A. Jemal, X.Q. Yu, J. He, Cancer statistics in China, 2015, CA Cancer J. Clin. 66 (2016) 115–132.
[5] X. Chen, Z. Chen, S. Yu, F. Nie, S. Yan, P. Ma, Q. Chen, C. Wei, H. Fu, T. Xu, S. Ren, Z. Wang, M. Sun, Long noncoding RNA LINC01234 functions as a competing endogenous RNA to regulate CBFB expression by sponging miR-204-5p in gastric cancer, Clin. Cancer Res. (2018).
[6] X. Chen, K. Zeng, M. Xu, X. Hu, X. Liu, T. Xu, B. He, Y. Pan, H. Sun, S. Wang, SP1-induced lncRNA-ZFAS1 contributes to colorectal cancer progression via the miR-150-5p/VEGFA axis, Cell Death Dis. 9 (2018) 982.
[7] G. Davuluri, W.P. Schiemann, E.F. Plow, K. Sossey-Alaoui, Loss of WAVE3 sensitizes triple-negative breast cancers to chemotherapeutics by inhibiting the STAT-HIF-1alpha-mediated angiogenesis, Jak-stat 3 (2014) e1009276.

[8] W.J. Ding, M. Zhou, M.M. Chen, C.Y. Qu, HOXB8 promotes tumor metastasis and the epithelial-mesenchymal transition via ZEB2 targets in gastric cancer, J. Cancer Res. Clin. Oncol. 143 (2017) 385–397.

[9] L. Fan, K. Strasser-Weippl, J.J. Li, J. St Louis, D.M. Finkelstein, K.D. Yu, W.Q. Chen, Z.M. Shao, P.E. Goss, Breast cancer in China, Lancet Oncol. 15 (2014) e279–289.

[10] J. Gu, Y. Wang, X. Wang, D. Zhou, C. Shao, M. Zhou, Z. He, Downregulation of lncRNA GAS5 confers tamoxifen resistance by activating miR-222 in breast cancer, Cancer Lett. 434 (2018) 1–10.

[11] M.D. Huang, W.M. Chen, F.Z. Qi, R. Xia, M. Sun, T.P. Xu, L. Yin, E.B. Zhang, W. De, Y.Q. Shu, Long non-coding RNA ANRIL is upregulated in hepatocellular carcinoma and regulates cell apoptosis by epigenetic silencing of KLF2, J. Hematol. Oncol. 8 (2015) 50.

[12] X. Huang, X. Xie, P. Liu, L. Yang, B. Chen, C. Song, H. Tang, X. Xie, Adam12 and lnc015192 act as ceRNAs in breast cancer by regulating miR-34a, Oncogene (2018).

[13] Y. Huang, B. Xiang, Y. Liu, Y. Wang, H. Kan, LncRNA CDKN2B-AS1 promotes tumor growth and metastasis of human hepatocellular carcinoma by targeting let-7c-5p/NAP1L1 axis, Cancer Lett. (2018).

[14] M.Z. Johnson, P.D. Crowley, A.G. Foley, C. Xue, C. Connolly, H.C. Gallagher, D.J. Buggy, Effect of perioperative lidocaine on metastasis after sevoflurane or ketamine-xylazine anaesthesia for breast tumour resection in a murine model, Br. J. Anaesth. 121 (2018) 76–85.

[15] A. Kapinova, P. Kubatka, P. Zubor, O. Golubnitschaja, Z. Dankova, S. Uramova, I. Pilchova, M. Caprnda, R. Opatrilova, J. Richnavsky, P. Kruzliak, J. Danko, The hypoxia-responsive long non-coding RNAs may impact on the tumor biology and subsequent management of breast cancer, Biomed. Pharmacother. 99 (2018) 51–58.

[16] X. Kong, Y. Duan, Y. Sang, Y. Li, H. Zhang, Y. Liang, Y. Liu, N. Zhang, Q. Yang, LncRNA-CDC6 promotes breast cancer progression and function as ceRNA to target CDC6 by sponging microRNA-215, J. Cell. Physiol. (2018).

[17] G.Y. Li, W. Wang, J.Y. Sun, B. Xin, X. Zhang, T. Wang, Q.F. Zhang, L.B. Yao, H. Han, D.M. Fan, A.G. Yang, L.T. Jia, L. Wang, Long non-coding RNAs AC026904.1 and UCA1: a "one-two punch" for TGF-beta-induced SNAI2 activation and epithelial-mesenchymal transition in breast cancer, Theranostics 8 (2018) 2846–2861.

[18] G.Y. Li, W. Wang, J.Y. Sun, B. Xin, X. Zhang, T. Wang, Q.F. Zhang, L.B. Yao, H. Han, D.M. Fan, A.G. Yang, L.T. Jia, L. Wang, Long non-coding RNAs AC026904.1 and UCA1: a "one-two punch" for TGF-β-induced SNAI2 activation and epithelial-mesenchymal transition in breast cancer, Theranostics 8 (2018) 2846–2861.

[19] L. Li, Y. Li, Y. Huang, Y. Ouyang, Y. Zhu, Y. Wang, X. Guo, Y. Yuan, K. Gong, The lncRNA MIF-AS1 promotes gastric cancer cell proliferation and reduces apoptosis to up-regulate NDUFA4, Cancer Sci. (2018).

[20] P. Li, G. Zhang, J. Li, R. Yang, S. Chen, S. Wu, F. Zhang, Y. Bai, H. Zhao, Y. Wang, S. Dun, X. Chen, Q. Sun, G. Zhao, Long noncoding RNA RGMB-AS1 indicates a poor prognosis and modulates cell proliferation, migration and invasion in lung adenocarcinoma, PLoS One 11 (2016) e0150790.

[21] X. Li, H. Lin, F. Jiang, Y. Lou, L. Ji, S. Li, Knock-down of HOXB8 prohibits proliferation and migration of colorectal Cancer cells via Wnt/beta-Catenin signaling pathway, Med. Sci. Monit. 25 (2019) 711–720.

[22] Z. Li, X. Zhao, Y. Zhou, Y. Liu, Q. Zhou, H. Ye, Y. Wang, J. Zeng, Y. Song, W. Gao, S. Zheng, B. Zhuang, H. Chen, W. Li, H. Li, H. Li, Z. Fu, R. Chen, The long non-coding RNA HOTTIP promotes progression and gemcitabine resistance by regulating HOXA13 in pancreatic cancer, J. Transl. Med. 13 (2015) 84.

[23] Y. Liang, X. Song, Y. Li, Y. Sang, N. Zhang, H. Zhang, Y. Liu, Y. Duan, B. Chen, R. Guo, W. Zhao, L. Wang, Q. Yang, A novel long non-coding RNA-PRLB acts as a tumor promoter through regulating miR-4766-5p/SIRT1 axis in breast cancer, Cell Death Dis. 9 (2018) 563.

[24] P.H. Lin, M.H. Yeh, L.C. Liu, C.J. Chen, Y.C. Tsui, C.H. Su, H.C. Wang, J.A. Liang, H.W. Chang, H.S. Wu, S.P. Yeh, L.Y. Li, C.F. Chiu, Clinical and pathologic risk factors of tumor recurrence in patients with node-negative early breast cancer after mastectomy, J. Surg. Oncol. 108 (2013) 352–357.

[25] Y. Lin, W. Guo, N. Li, F. Fu, S. Lin, C. Wang, Polymorphisms of long non-coding RNA HOTAIR with breast cancer susceptibility and clinical outcomes for a southeast Chinese Han population, Oncotarget 9 (2018) 3677–3689.

[26] X. Liu, L. Bi, Q. Wang, M. Wen, C. Li, Y. Ren, Q. Jiao, J.H. Mao, C. Wang, G. Wei, Y. Wang, miR-1204 targets VDR to promotes epithelial-mesenchymal transition and metastasis in breast cancer, Oncogene (2018).

[27] M.H. Lü, B. Tang, S. Zeng, C.J. Hu, R. Xie, Y.Y. Wu, S.M. Wang, F.T. He, S.M. Yang, Long noncoding RNA BC032469, a novel competing endogenous RNA, upregulates hTERT expression by sponging miR-1207-5p and promotes proliferation in gastric cancer, Oncogene (2015).

[28] Y. Luo, J.J. Chen, Q. Lv, J. Qin, Y.Z. Huang, M.H. Yu, M. Zhong, Long non-coding RNA NEAT1 promotes colorectal cancer progression by competitively binding miR-34a with SIRT1 and enhancing the Wnt/β-catenin signaling pathway, Cancer Lett. (2018).

[29] C.P. Ponting, P.L. Oliver, W. Reik, Evolution and functions of long noncoding RNAs, Cell 136 (2009) 629–641.

[30] Y. Shi, J. Li, Y. Liu, J. Ding, Y. Fan, Y. Tian, L. Wang, Y. Lian, K. Wang, Y. Shu, The long noncoding RNA SPRY4-IT1 increases the proliferation of human breast cancer cells by upregulating ZNF703 expression, Mol. Cancer 14 (2015) 51.

[31] R.L. Siegel, K.D. Miller, A. Jemal, Cancer statistics, 2016, CA Cancer J. Clin. 66 (2016) 7–30.

[32] K.P. Sorensen, M. Thomassen, Q. Tan, M. Bak, S. Cold, M. Burton, M.J. Larsen, T.A. Kruse, Long non-coding RNA HOTAIR is an independent prognostic marker of metastasis in estrogen receptor-positive primary breast cancer, Breast Cancer Res. Treat. 142 (2013) 529–536.

[33] C. Sun, S. Li, F. Zhang, Y. Xi, L. Wang, Y. Bi, D. Li, Long non-coding RNA NEAT1 promotes non-small cell lung cancer progression through regulation of miR-377-3p-E2F3 pathway, Oncotarget (2016).

[34] K. Tano, N. Akimitsu, Long non-coding RNAs in cancer progression, Front. Genet. 3 (2012) 219.

[35] L.A. Torre, F. Bray, R.L. Siegel, J. Ferlay, J. Lortet-Tieulent, A. Jemal, Global cancer statistics, 2012, CA Cancer J. Clin. 65 (2015) 87–108.

[36] I. Ulitsky, D.P. Bartel, lincRNAs: genomics, evolution, and mechanisms, Cell 154 (2013) 26–46.

[37] Y. Wang, C. Wu, C. Zhang, Z. Li, T. Zhu, J. Chen, Y. Ren, X. Wang, L. Zhang, X. Zhou, TGF-β-induced STAT3 overexpression promotes human head and neck squamous cell carcinoma invasion and metastasis through malat1/miR-30a interactions, Cancer Lett. (2018).

[38] O. Wapinski, H.Y. Chang, Long noncoding RNAs and human disease, Trends Cell Biol. 21 (2011) 354–361.

[39] W. Wu, F. Chen, X. Cui, L. Yang, J. Chen, J. Zhao, D. Huang, J. Liu, L. Yang, J. Zeng, Z. Zeng, Y. Pan, F. Su, J. Cai, Z. Ying, Q. Zhao, E. Song, S. Su, LncRNA NKILA suppresses TGF-β-induced epithelial-mesenchymal transition by blocking NF-κB signaling in breast Cancer, Int. J. Cancer (2018).

[40] Z. Xing, Y. Zhang, K. Liang, L. Yan, Y. Xiang, C. Li, Q. Hu, F. Jin, V. Putluri, N. Putluri, C. Coarfa, A. Sreekumar, P.K. Park, T.K. Nguyen, S. Wang, J. Zhou, Y. Zhou, J.R. Marks, D.H. Hawke, M.C. Hung, L. Yang, L. Han, H. Ying, C. Lin, Expression of long noncoding RNA YIYA promotes glycolysis in breast Cancer, Cancer Res. 78 (2018) 4524–4532.

[41] M. Xu, X. Chen, K. Lin, K. Zeng, X. Liu, B. Pan, X. Xu, T. Xu, X. Hu, L. Sun, B. He, Y. Pan, H. Sun, S. Wang, The long noncoding RNA SNHG1 regulates colorectal cancer cell growth through interactions with EZH2 and miR-154-5p, Mol. Cancer 17 (2018) 141.

[42] X. Yan, D. Zhang, W. Wu, S. Wu, J. Qian, Y. Hao, F. Yan, P. Zhu, J. Wu, G. Huang, Y. Huang, J. Luo, X. Liu, B. Liu, X. Chen, Y. Du, R.S. Chen, Z. Fan, Mesenchymal stem cells promote hepatocarcinogenesis via lncRNA-MUF interaction with ANXA2 and miR-34a, Cancer Res. (2017).

[43] X.Z. Yang, T.T. Cheng, Q.J. He, Z.Y. Lei, J. Chi, Z. Tang, Q.X. Liao, H. Zhang, L.S. Zeng, S.Z. Cui, LINC01133 as ceRNA inhibits gastric cancer progression by sponging miR-106a-3p to regulate APC expression and the Wnt/β-catenin pathway, Mol. Cancer 17 (2018) 126.

[44] J. Zhao, Y. Liu, W. Zhang, Z. Zhou, J. Wu, P. Cui, Y. Zhang, G. Huang, Long non-coding RNA Linc00152 is involved in cell cycle arrest, apoptosis, epithelial to mesenchymal transition, cell migration and invasion in gastric cancer, Cell Cycle 14 (2015) 3112–3123.

[45] Y. Zhao, Q. Guo, J. Chen, J. Hu, S. Wang, Y. Sun, Role of long non-coding RNA HULC in cell proliferation, apoptosis and tumor metastasis of gastric cancer: a clinical and in vitro investigation, Oncol. Rep. 31 (2014) 358–364.